Published in IET Microwaves, Antennas & Propagation
Received on 14th January 2013
Revised on 5th March 2013
Accepted on 17th March 2013
doi: 10.1049/iet-map.2013.0005

ISSN 1751-8725

Compact negative-epsilon stop-band structures based on double-layer chiral inclusions

Seyed Mohammad Hashemi[1], *Mohammad Soleimani*[1], *Sergei A. Tretyakov*[2]

[1]*Department of Electrical Engineering, Iran University of Science and Technology, Tehran, Iran*
[2]*Department of Radio Science and Engineering/SMARAD CoE, Aalto University, FI-00076 Aalto, Finland*
E-mail: hashemy@iust.ac.ir

Abstract: Here the authors propose to use electrically excited compact chiral resonators in microstrip configurations for realisation of weakly-radiating stop-band transmission lines. The fundamental resonant mode of these resonators can be excited by both electric and magnetic fields applied parallel to the spiral axis. The authors propose to use a racemic arrangement of an equal amount of left- and right-handed chiral particles between the ground plane and the signal strip and orient the particles so that they are excited by the electric field of the microstrip line. The advantage of this configuration (in addition to strong coupling and weak radiation from excited particles) is that the ground plane can be preserved from being etched (continuous ground structure). The other advantage is that the size of negative permittivity lines loaded with chiral particles can be made very small compared to previous implementations based on complementary split-ring resonators. The circuit models with properly extracted parameters accurately describe the behaviour of both negative permittivity and double-negative lines loaded with electrically coupled resonators. This parameter extraction technique is based on the comparison between the simulated (or measured) transmission and reflection characteristics of the host line loaded with such resonators and those obtained from its lumped-element equivalent circuit model.

1 Introduction

During recent years, split ring resonators (SRRs) [1] have attracted significant interest among experts in electromagnetics and microwave engineering because of potential applications in the synthesis of metamaterials with negative effective permeability based on periodic arrangements of these resonators [1, 2]. This functionality can be achieved in a narrow frequency band above the resonant frequency of SRRs and for magnetic-field vector applied parallel to the ring axis. The key to the success in the realisation of such artificial media is the fact that, in the vicinity of the resonance, SRR dimensions are small as compared to the signal wavelength. Therefore an array composed of these particles can be considered as an effective continuous medium with some effective electromagnetic parameters. The synthesis of negative-permeability media by means of SRRs opened the door to the design of metamaterials that are able to exhibit backward wave propagation and negative refractive index [2].

After these seminal works, several double-negative (DN) metamaterials based on SRRs in one-dimensional (1D) configurations were reported, including waveguide [3] and planar technologies [4], indicating the significance of these subwavelength resonators and their potentiality not only to verify the exotic electromagnetic properties of metamaterials predicted by Veselago [5], but also in the design of functional microwave devices with improved performance and reduced dimensions [6–9].

To achieve most of the relevant characteristics of metamaterials, the artificial structures must exhibit effective media properties. To this end, the constituent building blocks (SRRs etc.) must be electrically small, that is, with the dimensions significantly smaller than the signal wavelength at the frequencies of interest. As it was reported in [10], by combining two appropriately shaped metal elements at both sides of a dielectric layer connected by vias, it is possible to design new resonant particles with high level of miniaturisation (Fig. 1). The use of the proposed strategy for area reduction does not lead to a severe degradation in the quality factor [10]. These new resonators can also be potentially used to reduce the area of planar passive components, generating increasing interest in the synthesis of metamaterials transmission lines with extremely small unit cell sizes.

Usually, all of these miniaturised particles are excited by magnetic field and are magnetically coupled to the metamaterial transmission line (both microstrip lines and coplanar waveguides) [10–12]. They are able to inhibit signal propagation in the vicinity of the resonance and this stopband behaviour is because of inductive coupling between the line and the particles. Since the electrical size of the particles is small, these structures can be considered as artificial homogeneous transmission lines characterised by effective parameters, permeability μ_{eff} and permittivity

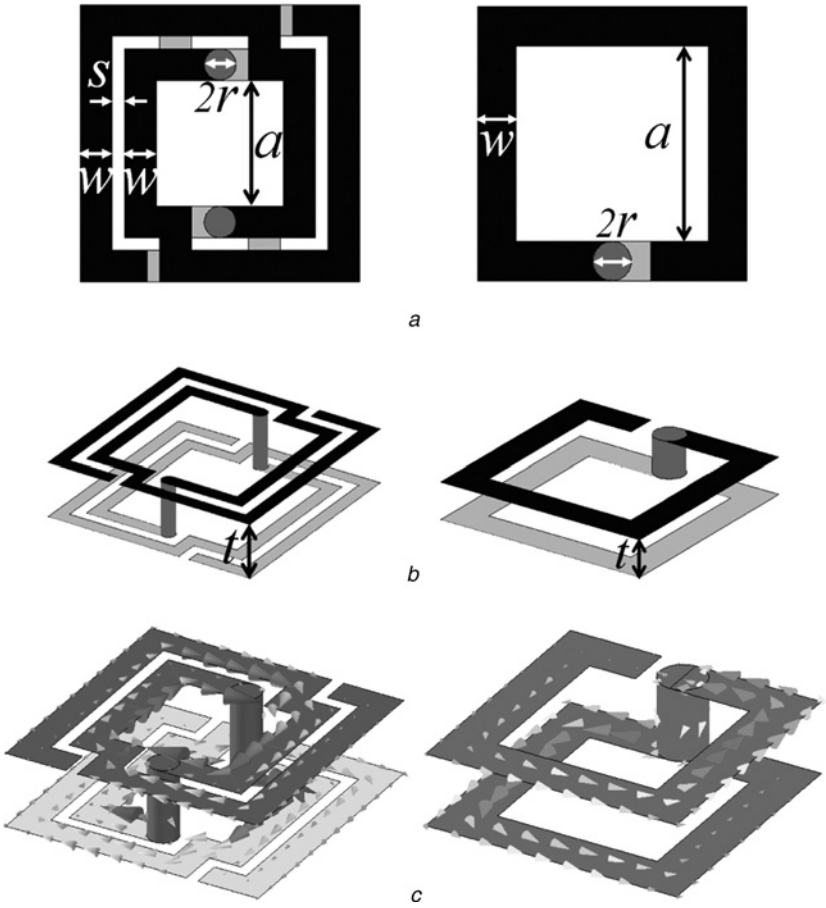

Fig. 1 *Topologies for metamaterial resonators with two metal levels (at both sides of a dielectric layer) connected by vias*

a Structure of BC-SR and BC-NB-SRR from right to left, top
b 3D views and relevant dimensions
c Results of full wave simulation of the induced currents in the resonators, obtained by electrically excitation with microstrip line

ε_{eff}. For magnetically loaded transmission lines μ_{eff} is negative/positive in a narrow band above/below resonance, and it takes extreme values near the resonance. For this reason, the typical stopband of these structures extends not only above the resonance, but also in a narrow band below it [4].

Another resonant element which can realise effective negative permittivity is the complementary SSR (CSRR) [13]. CSRRs are etched in the ground plane and the main driving mechanism is electric coupling by the electric field parallel to the axis of the rings. We know that in certain applications substrate is sustained by a metallic holder and also defected ground structures can lead to some electromagnetic compatibility (EMC) problems. This problem also exists for microstrip lines loaded with miniaturised two metal layers particles excited with magnetic field, because it is imperative to open windows in the ground plane in order to etch the lower side of the particle and excite it with magnetic field effectively [10, 12, 14].

2 Proposed configuration

One idea for reducing radiation from stop-band structures based on CSRR is to add an extra grounded layer under the original CSRR structure to form a new continuous ground, so that possible EMC problems can be avoided. However, simulations of such improved CSRR structure show that the added grounded layer degrades the CSRR performance (decreasing the rejection level and increasing losses). These results are illustrated in Fig. 2. The results are based on the assumption that there is free space between the added ground layer and an original CSRR. If we insert a dielectric putted between these two layers, then the performance degradation is stronger than in Fig. 2 (not shown here for brevity).

Thus, we propose a different layout, utilising the electromagnetic properties of chiral particles. We use the resonators with two metal layers connected by vias, which have chiral (Fig. 1) shape. The fundamental magnetic mode can be excited by both electric and magnetic fields applied parallel to the ring axis [15–17]. The susceptibility to electric field is because of the strong electric field between the upper and lower rings that appear near the resonance. Depending on whether the excitation produced through the electric or the magnetic field, such coupling to transmission line is identified as electric or magnetic. Previously, chiral inclusions have been used mainly in the design of volumetric or planar metamaterials, for example [14, 15, 17]. Earlier work on spiral inclusions coupled to transmission lines see in [12] (magnetically-coupled resonators).

As is known from the theory of artificial chiral media, the magneto–electric coupling effect (excitation of magnetic mode by external electric field) in electrically small

doi: 10.1049/iet-map.2013.0005

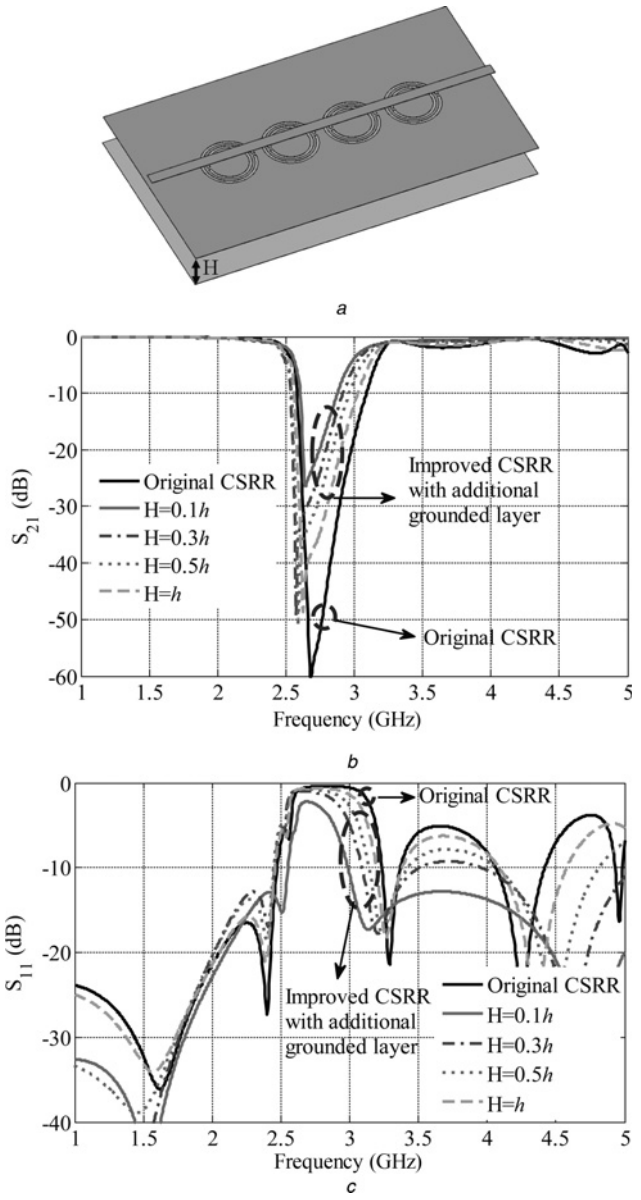

Fig. 2 *Layout of four improved CSRR structure with additional grounded layer to form a new continuous ground*

a By which the possible EMC problem can be avoided
b Frequency response (transmission S_{21} coefficient)
c (Reflection S_{11} coefficient) depicted in a decibel scale
The considered substrate is Rogers RO3010 with thickness $h = 1.27$ mm, dielectric constant $\varepsilon_r = 10.2$, $\tan\delta = 0.0022$ and deposited copper thickness 35 μm with bulk conductivity $\sigma = 5.6 \times 10^7$ S/m. The CSRR [13] dimensions are $c = d = 0.3$ mm, $r = 3.0$ mm and the periodicity is 7 mm

particles is much stronger than excitation of the same mode by external magnetic field. Although the chirality effect is linearly proportional to the electrical size of the particle, the magnetic effect is proportional to the second power of this parameter (e.g. [16, 17]). Our suggestion is to use a racemic mixture (with an equal amount of left- and right-handed inclusions) of chiral particles in microstrip lines for electric excitation of fundamental magnetic mode of compact resonators. Orienting particle's metal layers parallel to the ground plane, a significant component of the electric line field is parallel to the rings' axis, as desired. This arrangement is expected to allow strong coupling in compact configurations and allow applications where the induced strong but weakly-radiating magnetic moments can be used, for example, in sensing magnetic substances. Racemic arrangement (equal number of left- and right-handed inclusions) of electrically densely packed inclusions further minimises radiation from induced magnetic moments. In more conventional applications (like filters) these particles can be used in the substrate as embedded-circuit metamaterial inclusions between the ground plane and the signal strip. The advantage of this configuration (in addition to strong coupling and weak radiation from excited particles) is that the ground plane can be preserved from being etched (continuous ground structure). The other advantage (illustrated in Fig. 3) is that the size of negative permittivity lines loaded with broadside coupled spiral resonators (BC-SRs) can be made actually very small compared to the known implementations based on CSRR. However, it should be taken into account that for these resonators with two metal layers, four metal layers are necessary: two for the resonator and two for the microstrip line (Fig. 4*c*). Also, the rejection bandwidth for two metal layers resonators is narrower and with more loss. The geometric tailoring for loss reduction considered in Section 3.3.

It is well known that the current distribution in a resonator near its resonances does not significantly depend on the excitation and the electric excitation of these resonators excites the fundamental resonant mode (the quasi-static resonance). To verify the electromagnetic properties of these resonators, full-wave simulations have been performed and the surface current distributions because of the electric excitation for the analysed resonances are obtained. Simulation results show that electric excitation indeed induces current loops at the fundamental resonance

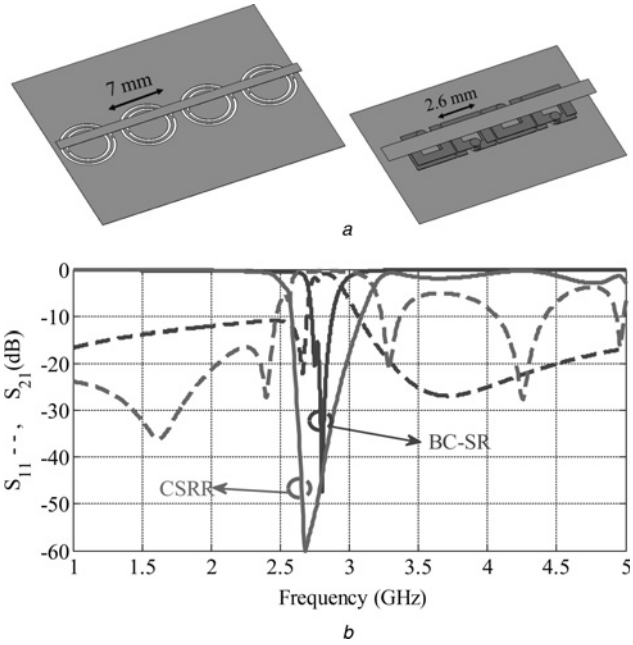

Fig. 3 *Layout of four BC-SRs and four CSRRs*

a From right to left loaded microstrip line structure
b Frequency response (reflection, S_{11} - - , and transmission, S_{21}, coefficients) depicted in a decibel scale
The considered substrate is Rogers RO3010 with thickness $h = 1.27$ mm, $\tan\delta = 0.0022$ and deposited copper thickness 35 μm with bulk conductivity $\sigma = 5.6 \times 10^7$ S/m. The dimensions of the BC-SR are $a = 1.2$ mm, $w = 0.65$ mm, $t = 1.27 \div 3$ mm and $2r = 0.65$ mm and the conductor microstrip width is $W_m = 1.2$ mm. The CSRR [13] dimensions are $c = d = 0.3$ mm, $r = 3.0$ mm and the periodicity is 7 mm

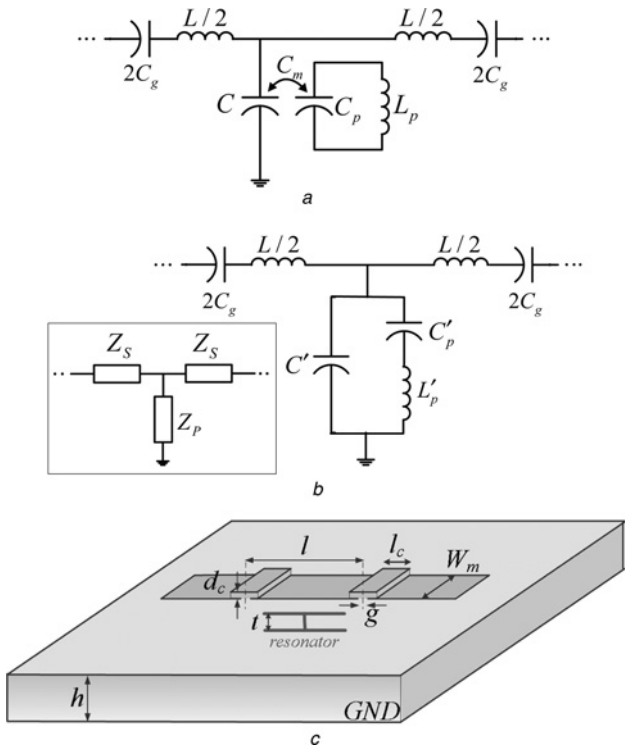

Fig. 4 *Lumped element equivalent circuit for the basic DN unit cell*

a Layouts of electrically coupled unit cells corresponding microstrip lines
b Transformed T-circuit model of the basic DN cell
c Layouts of the considered microstrip structures combining two metal levels connected by vias resonators with series gaps

(Fig. 1*c*). Study of the different resonant modes and the corresponding current distributions can be found in [18]. The electric excitation provides an effective negative permittivity, rather than permeability and for avoiding chirality effect we can use a racemic configuration of particles or a racemic arrangement of chiral inclusions. In general, these types of resonators can be implemented in 2D arrays, as an embedded-circuit metamaterial, for providing a uniaxial substrate. This case will be considered in a separate work.

In this paper, we study the effect of electrically excited resonators with two metal layers connected by vias, on the effective media properties of 1D metamaterial transmission line and propose a method for finding the electrical characteristics of metamaterial resonators coupled to planar transmission lines. As will be shown, the introduced circuit models with properly extracted parameters accurately describe the behaviour of these metamaterial transmission lines. Similar work for extracting the circuit parameters of metamaterial transmission lines loaded with SRRs or with other resonators magnetically coupled to the line has been published in [11] and for CSRRs electrically coupled to the line in [19, 20]. As illustrated in [11], the resonant particles can be modelled by *LC* tanks and, for the present case, their electric coupling to microstrip transmission line is modelled by a mutual capacitance (Fig. 4*a*). The circuit model presented here can be used for different resonators like BC-SRs, broadside coupled non-bianisotropic SRR (BC-NB-SRR) and other resonators with two metal levels connected by vias, excited by electric field for the analysis of the fundamental resonant mode (the quasi-static resonance) and can be considered as lumped or quasi-lumped elements.

3 Equivalent circuit models for electrically loaded transmission lines

In this section, it is shown that two metal layers particles can be used for the design of metamaterial transmission lines. The host line for the implementation of the particles in one dimension is the microstrip line and the racemic mixture of these particles provides negative effective permittivity. If the goal is to achieve backward-wave propagation, further microstructuring is necessary, in order to obtain the required negative effective permeability. In the microstrip technology, series capacitive gaps can be used to implement the negative permeability.

Here we propose a method for extracting the circuit parameters of metamaterial transmission lines loaded with two metal layers resonators electrically coupled to the line. This parameter extraction technique is based on the comparison between the simulated (or measured) transmission and reflection characteristics of a host line loaded with such resonators and those obtained from its lumped-element equivalent circuit model. From the extracted parameters, it is concluded that the circuit models very accurately predict the frequency responses of the considered structures.

The model describing the unit cell of metamaterial transmission lines loaded with electrically coupled resonators and series capacitive gaps is depicted in Fig. 4. As the two metal layers resonators are mainly excited by the electric field of the line, this coupling can be modelled by a mutual capacitance between the line capacitance and the resonators capacitance, which are modelled as parallel *LC* tanks. In Figs. 4*a* and *b* the layouts of electrically coupled unit cells corresponding to DN microstrip lines and transformed T-circuit model of it, respectively, are depicted. The validity of the lumped-element model is limited to the small electrical size of the unit cells and the coupling between adjacent resonators is neglected. For modelling the coupling between adjacent resonators, we can use more accurate circuit analysis [21]. Also the modelling of losses and geometric tailoring for loss reduction is considered in Section 3.3.

In reference to Fig 4*a*, L and C are the per-section inductance and capacitance of the line, C_g models the capacitance of the gaps, the electrically coupled resonators are described by means of the resonant tank constituted by the inductance L_p and the capacitance C_p, and, finally, their electric coupling to the line is described by the mutual capacitance $C_{\rm m}$. By obtaining the equivalent impedance of the shunt branch, the circuit can be simplified to that shown in Fig. 4*b*, whereL_p', C_p' and C' are given by

$$L_p' = \frac{C_p^2 L_p}{C_{\rm m}^2} = \frac{C_p}{C_{\rm m}^2 \omega_0^2} \tag{1}$$

$$C_p' = \frac{C_{\rm m}^2}{C_p} = C_{\rm m}^2 L_p \omega_0^2 \tag{2}$$

$$C' = C - C_p' \tag{3}$$

with $\omega_0^2 = 1/(L_p C_p)$. The series and shunt impedances of the unit cell in Fig. 4*b* read

$$Z_{\rm S}(\omega) = \frac{{\rm j}\omega L}{2}\left(1 - \frac{\omega_{s,s}^2}{\omega^2}\right) \tag{4}$$

doi: 10.1049/iet-map.2013.0005

$$Z_P(\omega) = \frac{1}{\mathrm{j}\omega C'}\left(\frac{\omega^2 - \omega_{p,\mathrm{s}}^2}{\omega^2 - \omega_{p,\mathrm{o}}^2}\right) \tag{5}$$

where $\omega_{s,\mathrm{s}}$ (series impedance is equivalent to a short circuit), $\omega_{p,\mathrm{s}}$ (shunt impedance is equivalent to a short circuit) and $\omega_{p,\mathrm{o}}$ (shunt impedance is equivalent to an open circuit) are the resonant angular frequencies defined by

$$\omega_{s,\mathrm{s}}^2 = \frac{1}{LC_g} \tag{6}$$

$$\omega_{p,\mathrm{s}}^2 = \frac{1}{L'_p C'_p} \tag{7}$$

$$\omega_{p,\mathrm{o}}^2 = \frac{1}{L'_p C'_p} + \frac{1}{L'_p C'} \tag{8}$$

Next we study the parameter extraction for both negative permittivity and backward transmission lines corresponding to the line without and with series gaps in Sections 3.1 and 3.2, respectively.

3.1 Negative permittivity transmission line

In order to load a microstrip transmission line with two metal layers particles, and thus obtain a negative effective permittivity medium, it is necessary to use them in the substrate as an embedded-circuit metamaterial, between the ground plane and the signal strip, that is, in such a way that the electric field is parallel to the rings' axis. In this case the inclusions are able to inhibit signal propagation in the vicinity of the resonance and this stopband behaviour is because of the capacitive coupling between the line and the particles. For parameter extraction the number of parameters of the circuit model in Fig. 4*b* is four (without series gaps), and we need four conditions to univocally determine such parameters.

The frequency $f_{p,s}$ [expression (7)] can be easily obtained from the transmission coefficient S_{21} of the unit cell since at this frequency the parallel branch is equivalent to a short circuit and the whole power injected from the input port is reflected back to the source. Thus, the transmission coefficient nulls (zero transmission frequency) and $f_{p,s}$ can be easily identified from the representation of the transmission coefficient in a decibel scale (Fig. 5*b*, The dotted curves refer to the validation, which is described in Section 4).

Then from the representation of the reflection coefficient of a single unit cell, S_{11}, in the Smith chart, we can determine $\omega_{p,\mathrm{o}}$ [expression (8)]. That shunt impedance is equivalent to an open circuit from the intercept of S_{11} with the unit resistance circle. This is obvious since at this frequency the real part of the impedance seen from the ports is simply the impedance of the opposite port, that is, $Z_0 = 50\ \Omega$. Hence, S_{11} must be allocated in the unit resistance circle at $f_{p,\mathrm{o}}$, as illustrated in Fig. 5*a*. On the other hand, the reactance of the unit cell seen from the ports at $f_{p,\mathrm{o}}$, which can be inferred from the Smith chart, is (without series gaps)

$$\mathrm{j}X\left(\omega_{p,\mathrm{o}}\right) = 2Z_{\mathrm{S}}\left(\omega_{p,\mathrm{o}}\right) = \mathrm{j}\omega_{p,\mathrm{o}}L \tag{9}$$

Thus, the per-section inductance of the line (L) can be directly determined from (9). Another condition can be deduced from

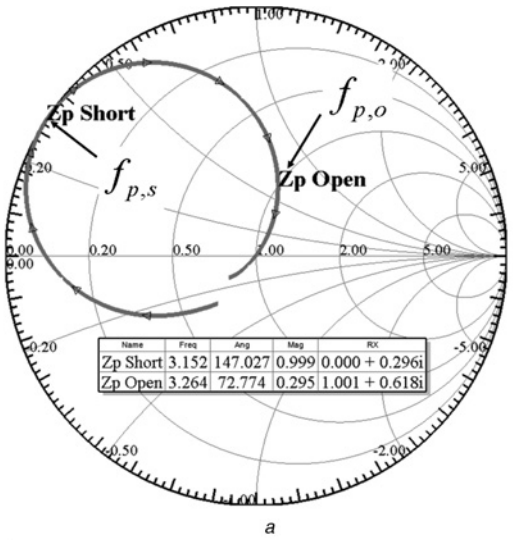

a

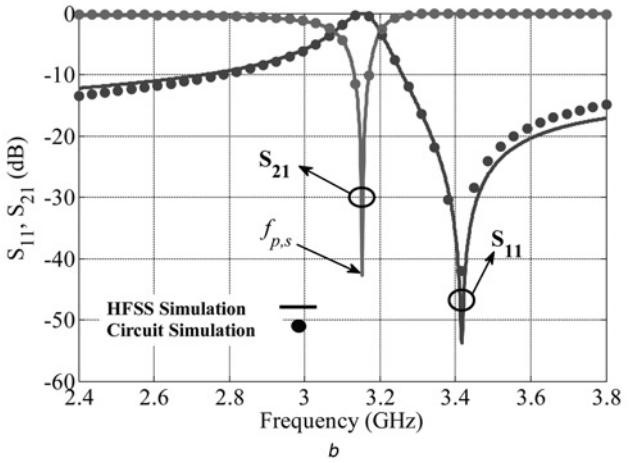

b

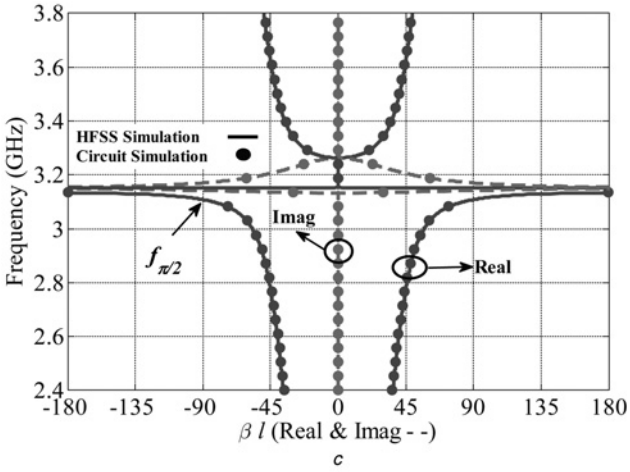

c

	C'_p(fF)	L'_p(nH)	C'(pF)	L(nH)
$\varepsilon < 0$	68.6	37.16	0.948	1.506

d

Fig. 5 *Reflection coefficient on the Smith chart*

a Frequency response (reflection, S_{11}, and transmission, S_{21}, coefficients) depicted in a decibel scale

b Dispersion relation

c Extracted element parameters

d Negative permittivity unit cell based on a microstrip structure

The considered substrate is Rogers RO3010 with thickness $h = 1.92$ mm. The dimensions of the BC-NB-SRR are $a = 1$ mm, $w = 0.25$ mm, $s = 0.1$ mm, $t = 0.64$ mm and $r = 0.125$ mm; and the conductor microstrip width is $W_{\mathrm{m}} = 2.2$ mm and the length $l = 3.2$ mm. The results of the circuit simulation with extracted parameters are depicted using symbols

the dispersion diagram. We can obtain the frequency ($f_{\pi/2}$) where the electrical length of the unit cell, $\phi = \beta l$ (β being the phase constant and l the length of the unit cell), is $\phi(f_{\pi/2}) = -90°$ (see Fig. 5*c*). Since the dispersion relation of a periodic structure consisting of cascaded unit cells, as those in Fig. 4*b*, is given by

$$\cos(\beta l) = 1 + \frac{Z_S}{Z_P} = \frac{1 - S_{11}S_{22} + S_{21}S_{12}}{2S_{21}} \tag{10}$$

with Z_S and Z_P being the series and shunt impedances, respectively, of the T-circuit model, and S_{ij} are the two-port scattering parameters, it follows that

$$\cos(\beta l = -90°) = 1 + \frac{Z_S(\omega_{\pi/2})}{Z_P(\omega_{\pi/2})} = 0 \rightarrow Z_S(\omega_{\pi/2}) = -Z_P(\omega_{\pi/2}) \tag{11}$$

with $\omega_{\pi/2} = 2\pi f_{\pi/2}$. Expressions (7)–(9) and (11) give four conditions needed to univocally determine the four circuit parameters (without series gaps) in Fig. 4

$$L = \frac{X(\omega_{p,o})}{\omega_{p,o}} \tag{12}$$

$$C' = \frac{2}{\omega_{\pi/2}^2 L}\left(\frac{\omega_{\pi/2}^2 - \omega_{p,s}^2}{\omega_{\pi/2}^2 - \omega_{p,o}^2}\right) \tag{13}$$

$$L'_p = \frac{1}{C'(\omega_{p,o}^2 - \omega_{p,s}^2)} \tag{14}$$

$$C'_p = \frac{1}{\omega_{p,s}^2 L'_p} \tag{15}$$

3.2 Backward transmission line

In order to synthesise an effectively DN medium, additional element able to provide the required negative effective permeability must be introduced to the structure. DN transmission line can be implemented by electrically loading a host line with two metal levels resonators and series capacitive gaps. These gaps make the structure behave as magnetic plasma, with negative valued permeability up to the plasma frequency that depends on the resonator formed by the gap capacitance and the per-section inductance of the line. Hence, to design a DN transmission line by combining two metal levels resonators and gaps it is necessary to design the structure so that the plasma frequency is higher than the resonance frequency of the particles. Under this condition there is a region where negative effective permeability and permittivity coexist.

For parameter extraction the number of parameters of the circuit model in Fig. 4*b* is five (with series gaps) and we also need five conditions to univocally determine such parameters. Indeed, by removing the series capacitive gaps, the per-section inductance of the line (L) can be directly determined from (9) and also by returning the series capacitive gaps, we can represent the corresponding reflection coefficient on a Smith chart and obtain the reactance seen from the ports at that frequency where S_{11} intercepts the unit resistance circle as (see Fig. 6*a*, As above, the dotted curves refer to the validation, see Section 4)

$$jX(\omega_{p,o}) = 2Z_S(\omega_{p,o}) = j\omega_{p,o}L + \frac{1}{j\omega_{p,o}C_g} \tag{16}$$

If we assume that the per-section inductance and capacitance of the line was not significantly changed by removing the series capacitive gaps, then we can univocally determine C_g from (16) and the other four parameters as explained previously from (12) to (15). However, this assumption is not exact and we may want to have a more accurate model. To find an accurate model for the structure with series gaps, we can compute the $\omega_{s,s}$ as a first approximation from (6) using the approximate L and C_g values. At this frequency ($f_{s,s}$), the series impedance (Z_S) is equivalent to a short circuit and the real part of the admittance seen from the ports is simply the admittance of the opposite port, that is, $Y_0 = (Z_0)^{-1} = (50\ \Omega)^{-1} = 0.02$S. Hence, S_{11} must be allocated in the unit conductance circle near $f_{s,s}$, as illustrated in Fig. 6*a*. Thus, the exact value of $\omega_{s,s} = 2\pi f_{s,s}$ can be obtained from the Smith chart. Note that we need the first approximation value of $\omega_{s,s}$ for finding the exact value from the Smith chart because S_{11} may be allocated in the unit conductance circle several times. Now (6) and (16) as two exact equations (based on simulation or measurement), can be used for computing L and C_g

$$L = \frac{\omega_{p,o}X(\omega_{p,o})}{\omega_{p,o}^2 - \omega_{s,s}^2} \tag{17}$$

$$C_g = \frac{\omega_{p,o}^2 - \omega_{s,s}^2}{\omega_{s,s}^2 \omega_{p,o} X(\omega_{p,o})} \tag{18}$$

Also $f_{p,s}$ (rejection in S_{21}) and $f_{\pi/2}$ (dispersion diagram) can be obtained from the two-port scattering parameters. By using a similar method previously described for (11), C' can be obtained

$$C' = \frac{2}{L}\frac{\omega_{\pi/2}^2 - \omega_{p,s}^2}{(\omega_{\pi/2}^2 - \omega_{p,o}^2)(\omega_{\pi/2}^2 - \omega_{s,s}^2)} \tag{19}$$

The formulation for obtaining the value of L'_p and C'_p is similar to (14) and (15), respectively.

3.3 Losses modelling and reducing by geometric tailoring

The total loss level is mainly determined by the resonators (because of strong circulating currents). Thus, the loss can be taken into account by including a series resistance in the model, so that the resonator is described by means of a parallel tank, where C'_p and L'_p are the reactive elements and resistor R accounts for losses (Fig. 7*a*). To determine R, this parameter is swept till electrical simulations and electromagnetic simulations (or experimental data) for the frequency responses agree. In practice, this parameter is determined with a good accuracy from the transmission coefficient of the negative permittivity structure, since the rejection level is very sensitive to this parameter [20].

doi: 10.1049/iet-map.2013.0005

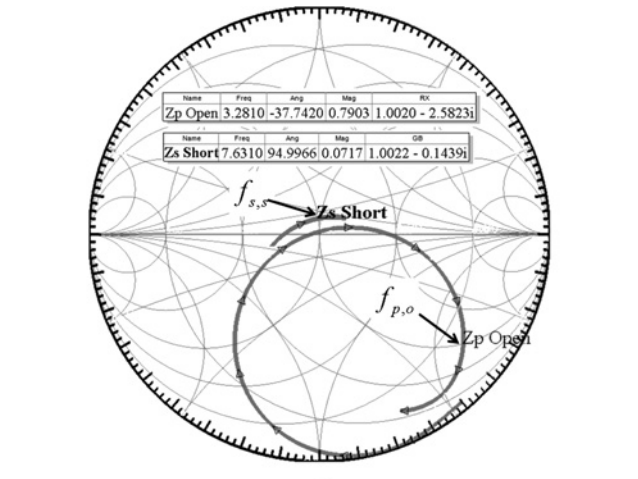

a

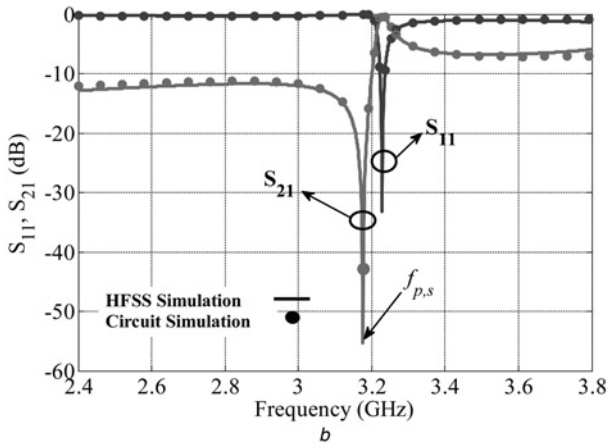

b

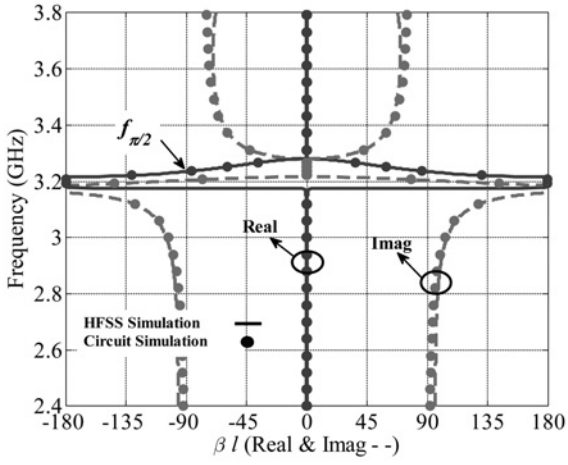

c

	C'_p(fF)	L'_p(nH)	C'(pF)	L(nH)	C_g(pF)
DN	63.3	39.65	0.942	1.42	0.306

d

Fig. 6 *Reflection coefficient on the Smith chart*

a Frequency response (reflection, S_{11}, and transmission, S_{21}, coefficients) depicted in a decibel scale
b Dispersion relation
c Extracted element parameters
d DN unit cell based on a microstrip structure
The considered substrate is Rogers RO3010 with thickness $h = 1.92$ mm. The dimensions of the BC-NB-SRR are $a = 1$ mm, $w = 0.25$ mm, $s = 0.1$ mm, $t = 0.64$ mm and $r = 0.125$ mm; and the conductor microstrip width is $W_m = 2.2$ mm and the length $l = 3.2$ mm. The dimensions of metal series gap are $g = 0.2$ mm, $d_c = 0.13$ mm and $l_c = 0.5$ mm with the same substrate. The results of the circuit simulation with extracted parameters are depicted using symbols

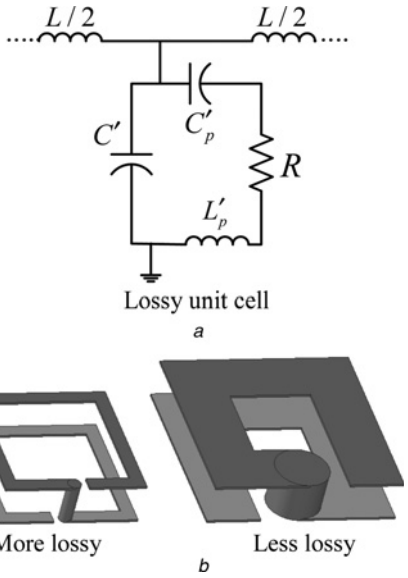

Fig. 7 *Lumped element equivalent circuit for the lossy unit cell (losses can be taken into account by including a series resistance in the model)*

a 3D view
b Of two BC-SR resonators with same resonant frequency but different loss

Losses in metamaterials render the applications of such exotic materials less practical unless an efficient way of reducing them is found. A loss reduction technique could be proposed based on geometric tailoring of the individual resonators. The loss of the structure could be further reduced by increasing conductor cross-section (Fig. 7*b*). The simulations results of two particles (the two sets of element dimensions have been chosen to yield the same resonance frequency) and the extracted element parameters are depicted in Fig. 8.

4 Validation of the model and results

The presented method has been applied to extracting the circuit model parameters (Fig. 4*b*) of different structures (Fig. 1). In this section, we will illustrate the validity of both the model and the parameter extraction method applying the technique to a microstrip line with a negative permittivity and a DN structures. The microstrip line is electrically loaded with a BC-NB-SRR as depicted in Fig. 4*c*. The dimensions of the BC-NB-SRR are (in reference to Fig. 1) $a = 1$ mm, $w = 0.25$ mm, $s = 0.1$ mm, $t = 0.64$ mm and $r = 0.125$ mm; and the conductor microstrip width is $W_m = 2.2$ mm and the length $l = 3.2$ mm (in reference to Fig. 4*c*). The considered substrate is Rogers RO3010 with the thickness $h = 3 \times 0.64$ mm and dielectric constant $\varepsilon_r = 10.2$.

The reflection coefficient of the structure (obtained from full-wave electromagnetic simulation by means of the HFSS commercial software) is depicted on a Smith chart in Fig. 5*a* and both the reflection and transmission coefficients are simultaneously depicted in the decibel scale in Fig. 5*b*. The dispersion diagram (also obtained from full-wave electromagnetic simulation) is depicted in Fig. 5*c*. We have applied the parameter extraction technique to this structure. From the extracted parameters, we have obtained the frequency response (reflection and transmission coefficients

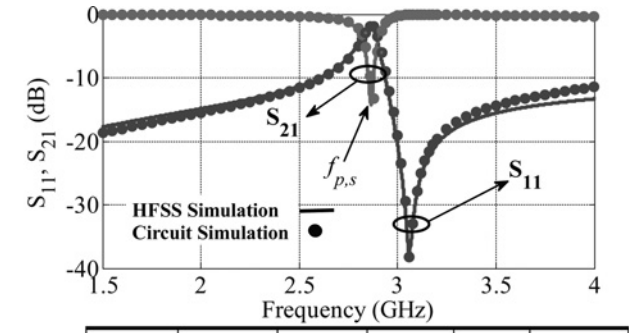

	C'_p(fF)	L'_p(nH)	C'(pF)	L(nH)	R(Ω)	S_{11}(dB)
$\varepsilon < 0$	58.66	52.27	0.954	1.39	6.3	-1.88

a

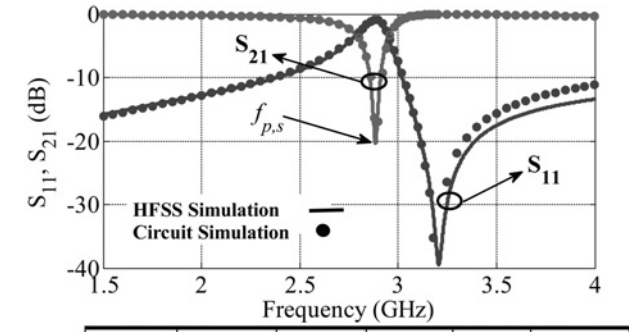

	C'_p(fF)	L'_p(nH)	C'(pF)	L(nH)	R(Ω)	S_{11}(dB)
$\varepsilon < 0$	116.3	26.07	1.01	1.31	2.85	-0.89

b

Fig. 8 *Frequency response (reflection, S_{11}, and transmission, S_{21}, coefficients) depicted in a decibel scale and extracted element parameters for two BC-SR resonators with dimensions*

a $a = 1.7$ mm, $w = 0.2$ mm, $t = 0.64$ mm and $r = 0.1$ mm (More lossy)
b $a = 1.2$ mm, $w = 0.8$ mm, $t = 0.64$ mm and $r = 0.4$ mm (Less lossy)
The considered substrate is Rogers RO3010 with thickness $h = 1.92$ mm, $\tan\delta = 0.0022$ and deposited copper thickness 35 µm with bulk conductivity $\sigma = 5.6 \times 10^7$ S/m. The conductor microstrip width is $W_m = 2.2$ mm and the length $l = 3.2$ mm

and phase response) from the electrical simulation of the circuit model. The results of these circuit simulations are also depicted in Fig. 5 to be easily comparable with the results obtained from the electromagnetic simulation of the layout. As can be appreciated, the circuit model describes the behaviour of the BC-NB-SRR in Fig. 1 with excellent accuracy (the circuit and electromagnetic simulations in Fig. 5 are hardly distinguishable). This confirms the validity of the model and the ability of the the reported technique to provide the circuit parameters of the structure.

The stopband behaviour is because of the capacitive coupling between the line and the particles. For transmission lines electrically loaded with a racemic mixture of particles, ε_{eff} is negative/positive in a narrow band above/below resonance, and it takes extreme values near the resonance. For this reason, the typical stopband of these structures extends not only above the resonance, but also in a narrow band below it.

To further exemplify the parameter extraction method, it has been applied for the BC-NB-SRR with a series gap in the microstrip structure. To achieve appropriate series capacitance parallel-plate (or lamp) capacitors can be implemented. The metal caps drastically enhance the capacitance to the adjacent cells and, consequently, the DN response is enhanced (see Fig. 4*c*). The electrical and electromagnetic simulations of the structure are depicted in Fig. 6. The dimensions of metal series gap are $g = 0.2$ mm, $d_c = 0.13$ mm and $l_c = 0.5$ mm with the same substrate. Again, the agreement between circuit and electromagnetic simulations is excellent. The corresponding dispersion diagram is depicted in Fig. 6*c*. The dispersion diagram exhibit a DN band characterised by antiparallel phase and group velocities. This double negative pass band appears in Fig. 6*b* after a rejection in S_{21} (because of particle resonance) as expected. Thus, we have backward wave propagation in the pass band.

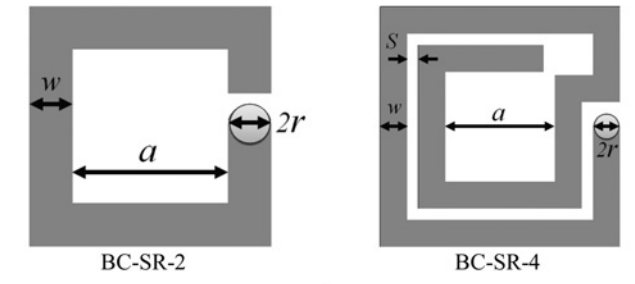

a

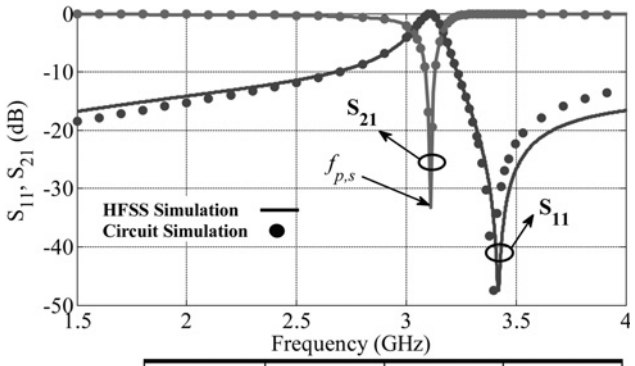

	C'_p(fF)	L'_p(nH)	C'(pF)	L(nH)
$\varepsilon < 0$	81.69	32.03	0.965	1.462

b

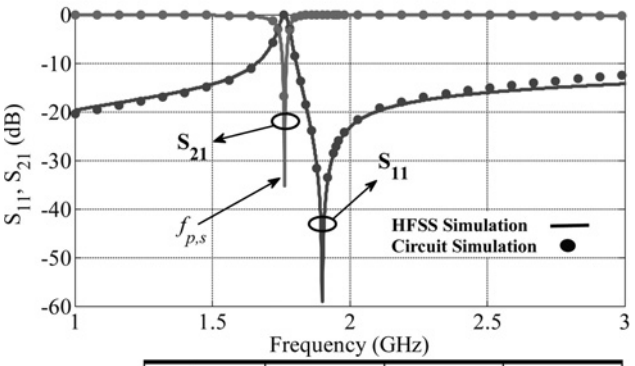

	C'_p(fF)	L'_p(nH)	C'(pF)	L(nH)
$\varepsilon < 0$	80.25	101.5	1.06	1.466

c

Fig. 9 *Topologies of the different resonators considered: BC-SR2 and BC-SR4*

a Frequency response (reflection, S_{11}, and transmission, S_{21}, coefficients) depicted in a decibel scale
b Extracted element parameters for two different resonators: BC-SR2
c BC-SR4 coupled to a microstrip structure
The considered substrate is Rogers RO3010 with thickness $h = 1.92$ mm. The dimensions of the BC-SR2 are $a = 1.4$ mm, $w = 0.4$ mm, $t = 0.64$ mm and $r = 0.2$ mm and the dimensions of the BC-SR4 are $a = 1$ mm, $w = 0.25$ mm, $s = 0.1$ mm, $t = 0.64$ mm and $r = 0.125$ mm and the conductor microstrip width is $W_m = 2.2$ mm and the length $l = 3.2$ mm. The results of the circuit simulation with extracted parameters are depicted using symbols

doi: 10.1049/iet-map.2013.0005

In order to demonstrate the viability of the proposed technique in Section 3.3, we have applied it to the determination of the electrical parameters of two BC-SRs of Fig. 7*b*. Dimensions of two BC-SRs resonators are: $a = 1.7$ mm, $w = 0.2$ mm, $t = 0.64$ mm and $r = 0.1$ mm (Fig. 8*a*), $a = 1.2$ mm, $w = 0.8$ mm, $t = 0.64$ mm and $r = 0.4$ mm (Fig. 8*b*). The two sets of element dimensions have been chosen to yield the same resonance frequency. The considered substrate is Rogers RO3010 with the thickness $h = 1.92$ mm, $\tan\delta = 0.0022$ and deposited copper thickness 35 μm with bulk conductivity $\sigma = 5.6 \times 10^7$ S/m. The conductor microstrip width is $W_m = 2.2$ mm and the length $l = 3.2$ mm. In Fig. 8 we plot the results of circuit and electromagnetic simulations of the reflection and transmission coefficients. Following the procedure described in the previous section, we have obtained the electrical parameters for both resonators by using the electromagnetic simulation data. With these element values, we have performed the circuit simulation of the frequency responses of the structures. The results are also included in Fig. 8 and very good agreement between electromagnetic and electrical simulations has been obtained in all the cases, which is indicative of the validity of both the model and the proposed method for parameter extraction of lossy unit cells.

In order to generalise the model and the parameter extraction technique, a microstrip line has been loaded with some different subwavelength resonators. The resonators that have been studied are BC-SRs with two turns (BC-SR-2), and BC-SRs with four turns (BC-SR-4). Fig. 9 shows the topologies of these two resonators, and the frequency response obtained from electromagnetic simulations together with the electrical response corresponding to the circuit obtained from the parameter extraction. These results demonstrate that the parameter extraction method is suitable for any two metal levels connected by vias subwavelength resonators, excited electrically.

5 Conclusions

In summary, we have introduced compact chiral and racemic dual-layer particles as electrically excited inclusions embedded in a microstrip line. In this configuration, the fundamental mode of the inclusion is characterised by strong induced magnetic moment (circulating currents), but in contrast to conventional split-ring configurations the mode is excited by the electric field of the line. This ensures strong excitation effect in a compact layout. Induced magnetic moments do not couple to the microstrip magnetic field and radiate weakly because of their positioning inside the line. In the considered examples we have demonstrated stop-band behaviour and backward-wave propagation in the structure. Strong local magnetic fields in the particle volume can be further exploited for sensing magnetic substances or for realisation of coupled waveguides or mode transformers.

Based on the comparisons of simulated and modelled responses of the structure we can conclude that the developed circuit model appropriately describes the behaviour of both negative permittivity and DN lines loaded with electrically coupled resonators. The developed parameter extraction method is simple and has been found useful for the characterisation of these metamaterial transmission lines.

6 Acknowledgments

Part of this work was done during the visit of the first author to Aalto University (Finland), which has been partially funded by the Academy of Finland and Nokia through the center-of-excellence program. The first author also would like to thank MSRT (The Ministry of Science, Research and Technology) and ITRC (Iran Telecommunications Research Center) for their financial support during the visit period.

7 References

1 Pendry, J.B., Holden, A.J., Robbins, D.J., Stewart, W.J.: 'Magnetism from conductors and enhanced nonlinear phenomena', *IEEE Trans. Microw Theory Tech.*, 1999, **47**, pp. 2075–2084
2 Smith, D.R., Padilla, W.J., Vier, D.C., Nemat-Nasser, S.C., Schultz, S.: 'Composite medium with simultaneously negative permeability and permittivity', *Phys. Rev. Lett.*, 2000, **84**, pp. 4184–4187
3 Marqués, R., Martel, J., Mesa, F., Medina, F.: 'Left-handed-media simulation and transmission of EM waves in subwavelength split-ring-resonator-loaded metallic waveguides', *Phys. Rev. Lett.*, 2002, **89**, pp. 183901
4 Martin, F., Bonache, J., Falcone, F., Sorolla, M., Marques, R.: 'Split ring resonator-based left-handed coplanar waveguide', *Appl. Phys. Lett.*, 2003, **83**, pp. 4652–4654
5 Veselago, V.G.: 'The electrodynamics of substances with simultaneously negative values of ε and μ', *Sov. Phys. Usp*, 1968, **10**, (4), pp. 509–514
6 Falcone, F., Martin, F., Bonache, J., *et al*: 'Left handed coplanar waveguide band pass filters based on bi-layer split ring resonators', *IEEE Microw. Wirel. Compon. Lett.*, 2004, **14**, pp. 10–12
7 Bonache, J., Gil, I., Garcia-Garcia, J., Martin, F.: 'Novel microstrip bandpass filters based on complementary split-ring resonators', *IEEE Trans. Microw. Theory Tech.*, 2006, **54**, pp. 265–271
8 Gil, M., Bonache, J., Garcia-Garcia, J., Martel, J., Martin, F.: 'Composite right/left-handed metamaterial transmission lines based on complementary split-rings resonators and their applications to very wideband and compact filter design', *IEEE Trans. Microw. Theory Tech.*, 2007, **55**, pp. 1296–1304
9 Duran-Sindreu, M., Velez, A., Aznar, F.: 'Applications of open split ring resonators and open complementary split ring resonators to the synthesis of artificial transmission lines and microwave passive components', *IEEE Trans. Microw. Theory Tech.*, 2009, **57**, pp. 3395–3403
10 Aznar, F., García-García, J., Gil, M., Bonache, J., Martín, F.: 'Strategies for the miniaturization of metamaterial resonators', *Microw. Opt. Technol. Lett.*, 2008, **50**, pp. 1263–1270
11 Aznar, F., Gil, M., Bonache, J., *et al*: 'Characterization of miniaturized metamaterial resonators coupled to planar transmission lines through parameter extraction', *J. Appl. Phys.*, 2008, **104**, pp. 114501
12 Aznar, F., Gil, M., Bonache, J., Garcia-Garcia, J., Martin, F.: 'Metamaterial transmission lines based on broad-side coupled spiral resonators', *Electron. Lett.*, 2007, **43**, pp. 530–532
13 Falcone, F., Lopetegi, T., Baena, J.D., *et al*: 'Effective negative-epsilon; stopband microstrip lines based on complementary split ring resonators', *IEEE Microw. Wirel. Compon. Lett.*, 2004, **14**, pp. 280–282
14 Baena, J.D., Marqués, R., Medina, F., Martel, J.: 'Artificial magnetic metamaterial design by using spiral resonators', *Phys. Rev. B*, 2004, **69**, pp. 014402
15 Marqués, R., Jelinek, L., Mesa, F.: 'Negative refraction from balanced quasi-planar chiral inclusions', *Microw. Opt. Technol. Lett.*, 2007, **49**, pp. 2606–2609
16 Serdyukov, A.N., Semchenko, I.V., Tretyakov, S.A., Sihvola, A.: 'Electromagnetics of bi-anisotropic materials: theory and applications' (Gordon and Breach Science Publishers, Amsterdam, 2001)
17 Tretyakov, S., Sihvola, A., Jylhä, L.: 'Backward-wave regime and negative refraction in chiral composites', *Photonics Nanostruct. Fundamentals Applic.*, 2005, **3**, pp. 107–115
18 Garcia-Garcia, J., Martin, F., Baena, J.D., *et al*: 'On the resonances and polarizabilities of split ring resonators', *J. Appl. Phys.*, 2005, **98**, p. 033103
19 Baena, J.D., Bonache, J., Martin, F., *et al*: 'Equivalent-circuit models for split-ring resonators and complementary split-ring resonators coupled to planar transmission lines', *IEEE Trans. Microw. Theory Tech.*, 2005, **53**, pp. 1451–1461
20 Bonache, J., Gil, M., Gil, I., *et al*: 'On the electrical characteristics of complementary metamaterial resonators', *IEEE Microw. Wirel. Compon. Lett.*, 2006, **16**, pp. 543–545
21 Gil, I., Bonache, J., Gil, M., *et al*: 'Accurate circuit analysis of resonant-type left handed transmission lines with inter-resonator coupling', *J. Appl. Phys.*, 2006, **100**, p. 074908